Superplastic behavior of a 7055 aluminum alloy

R. Kaibyshev[a], T. Sakai[b], F. Musin[a*], I. Nikulin[a], and H. Miura[b]

[a]*Institute for Metals Superplasticity Problems, Russian Academy of Sciences, Khalturina 39, Ufa 450001, Russia*
[b]*Department of Mechanical and Control Engineering, The University of Electro-Communications, Chofu, Tokyo 182-8585, Japan*

Abstract

It is shown that a high strength 7055 aluminum alloy with partially recrystallized initial structure exhibits superplastic behavior in the temperature interval 400–490 °C within a wide strain rate range from 8.3×10^{-5} to 3.3×10^{-2} s^{-1}. Maximum total elongation of about 960% and strain rate sensitivity coefficient, m, of 0.6 were obtained at a temperature of 450 °C and a strain rate of 3.3×10^{-4} s^{-1}.

Keywords: Aluminum alloys; High temperature mechanical properties; Microstructure; Continuous dynamic recrystallization

Introduction

Aerospace industry has a great interest in developing new high strength aluminum alloys. Aluminum alloy 7055 is a major candidate for such applications [1]. This alloy can be widely used instead of 7475 aluminum alloy. The perfect strength characteristics of 7055 alloy combine with sufficiently high fracture toughness, fatigue and corrosion resistance, ductility, which significantly exceed those of 7475 alloy. These advantages make efficient its application as structural material for upper wing elements. The 7055 alloy also exhibits excellent formability during conventional forging and extrusion, at elevated temperatures. In the same time, a low formability of sheets restricts the use of the 7055 alloy.

Superplastic forming (SPF) is an attractive manufacturing process which allows producing complex sheet-metal components. Developing a superplastic 7055 alloy would be useful for applications in fuselage skins or for other thin-walled components.

* Corresponding author.
E-mail address: fanil@anrb.ru (F. Musin).

Superplastic potential of aluminum alloys is critically dependent upon grain size, stability of fine grains at high temperature, and cavitation during SPF [2,3]. Microstructure suitable for SPF can be developed through thermomechanical processing (TMP). The phase composition of the 7055 alloy permits the use of overaging to develop large secondary precipitates ($\sim$1 μm) prior to cold rolling. Fine-grained microstructures can be formed by particle stimulated nucleation process during following recrystallization annealing [4,5]. This concept may be applied to make the 7055 alloy superplastic. Superplastic deformation of the 7055 alloy, however, has not been yet reported, systematically. The aim of this study is to report the superplastic behavior of the alloy subjected by a TMP. A specific attention will be paid to microstructure evolution and cavitation during superplastic deformation.

Experiments

The 7055 aluminum alloy with a chemical composition of Al–8.2%Zn–2.1%Mg–2.2%Cu–0.2%Zr (in wt.%) was manufactured by direct chill casting. The alloy was homogenized at 470 °C for 24 h and, subsequently, a two-step TMP was used for grain refinement.

(i) The 7055 alloy was rolled with a 70% reduction at 410 °C, followed by recrystallization annealing at 450 °C in salt bath for 1 h, and then quenched in water.
(ii) Next the overaging was performed at 410 °C for 4 h with a slow cooling to room temperature, followed by cold rolling with a 80% reduction. Final recrystallization annealing was carried out at 450 °C in a salt bath for 1 h.

Tensile tests were performed at temperatures ranging from 400 to 490 °C and strain rates ranging from 8.3×10^{-6} to 8.3×10^{-2} s^{-1}. An Instron universal testing machine (Model 1185) equipped with a three-zone split furnace was used. Temperature accuracy was within ±2 °C. The values of the strain rate sensitivity, m, were determined by strain-rate-jump tests [3].

Samples for metallographic examinations were prior electropolished using a 10%H_2ClO_4 solution in C_4H_9OH. Microstructures were revealed by etching with the standard Keller solution. Metallographic analysis was carried out using a Neophot-32 microscope and an Epiquant automated analysis equipment. The mean grain size was determined from measurements of more than 300 grains in longitudinal and transverse direction. For TEM examinations, samples were thinned to about 0.25 mm. Discs with 3 mm diameter were cut and electropolished to perforation with a Tenupol-3 twinjet polishing unit using a 20% nitric acid solution in methanol at −30 °C and 15 V. The thin foils were examined using a Jeol-2000EX TEM with a double-tilt stage at an accelerating potential of 200 kV.

Cavitation was measured in samples deformed to various strains using the standard point-count technique.

Results and discussion

Microstructure before deformation

The initial microstructure produced by the two-step TMP is shown in Fig. 1. It is clearly seen that there is a mixed structure composed of two structural components. One of them is the regions of recrystallized grains with an average size of about 11 μm and equiaxed shape. These grains are surrounded by high angle boundaries, and a large number of secondary phase particles were observed within these grains (Fig. 1b). The density of lattice dislocations is about $10^{12}\,m^{-2}$. Volume fraction of the recrystallized grains is about 64% (Fig. 1a).

The other regions comprise crystallites with a mean size of 2 μm, and their volume fraction is about 36% (Fig. 1a). TEM studies showed that boundaries of these crystallites have low angle misorientation (Fig. 1b). It can be concluded, therefore, that this structure is unrecrystallized and recovered subgrains. The density of secondary phase precipitates in the areas of these subgrains is less than that in the recrystallized areas mentioned above. Lattice dislocations are inhomogeneously distributed within subgrains, for instance, almost no lattice dislocations were revealed in some subgrains, and, in contrast, moderate dislocation density ($\rho = 10^{13}\ m^{-2}$) was found in other subgrains. Both recrystallized and unrecrystallized regions are distributed alternatively and parallel to prior rolling direction (Fig. 1a).

Mechanical properties

Typical true stress–true strain curves for the processed 7055 alloy at an initial strain rate of $\dot{\varepsilon} = 1.7 \times 10^{-3}\ s^{-1}$ and different temperatures (400–490 °C) and at a fixed temperature of 450 °C and different strain rates (8.3×10^{-5} to $8.3 \times 10^{-2}\ s^{-1}$) are presented in Fig. 2a and b, respectively. There is no apparent steady state flow at all temperatures and strain rates examined. Two types of σ–ε curves can be distinguished. After reaching

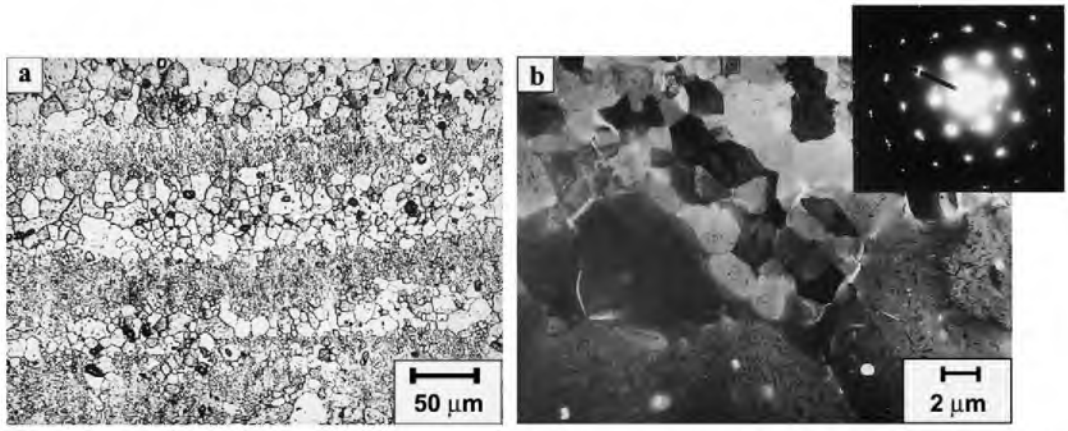

Fig. 1. Initial microstructure of the 7055 alloy after the two-step thermomechanical treatment: (a) optical and (b) TEM microstructures. The selected area electron diffraction patterns was taken from unrecrystallized structure.

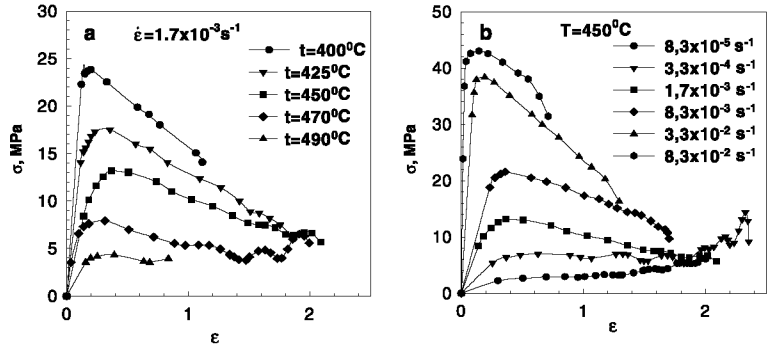

Fig. 2. Effect of temperature (a) and strain rate (b) on true stress–true strain curves for the 7055 Al.

a sharp stress peak, the flow stress decreases extensively until fracture at lower temperature (Fig. 2a) or at higher strain rates (Fig. 2b). Increasing temperature or decreasing strain rate leads to the shift of the peak stress to a higher strain. In contrast, a stress oscillation of flow curves appears at high temperature or at low strain rate. The stress oscillation is accompanied with a gradual strain hardening at high strains. Amplitude of stress oscillations tends to increase with strain. A transition from one to another type of true stress–true strain curves occurs at around 450 °C and $\dot{\varepsilon} = 1.7 \times 10^{-3}\ s^{-1}$.

The flow stress at a strain of 0.34 is plotted as a function of strain rate on a double logarithmic scale in Fig. 3a. A sigmoidal relationship is observed between stress and strain rate, especially at high testing temperatures, indicating three well-known deformation regions [2,3]. Fig. 3b and c represent variation of strain rate sensitivity, m, and elongation-to-failure, δ, with strain rate, respectively. At 450 °C, the maximum elongation-to-failure of 960% with a corresponding highest value of the strain rate sensitivity, m, of 0.6 was found at $\dot{\varepsilon} = 3.3 \times 10^{-4}\ s^{-1}$ (Fig. 3b and c). Both total elongation as well as m values tend to reduce on either side of this strain rate. It is concluded, therefore, that the present 7055 alloy behaves as a typical superplastic material in the

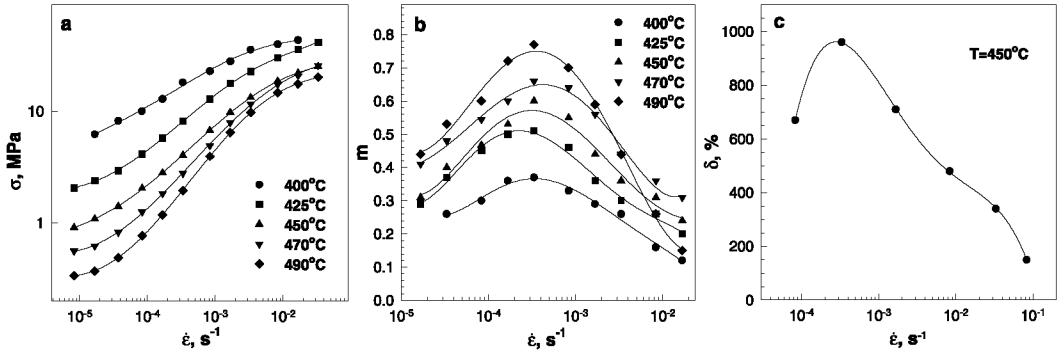

Fig. 3. Variations of flow stress (σ) (a), coefficient of strain rate sensitivity (m) (b) and elongation-to-failure (δ) (c) with strain rate.

temperature range 425–490 °C [2,3]. Notably, the total elongation exceeds 400% in the strain rate range 8.3×10^{-5}–8.3×10^{-3} s^{-1}, and decreases at higher strain rates at 450 °C (Fig. 3c). For example, at $\dot{\varepsilon} = 8.3 \times 10^{-2}$ s^{-1} the total elongation is only 150% despite of similarity in m values. It is caused by the fact that elongation-to-failure depends on uniformity of plastic flow which tends to growth with increasing both the strain rate sensitivity as well as strain hardening [3]. Strain softening yielding strain localization at the high strain rates and the low temperatures results in reduced plasticity resource.

Tensile elongation-to-failure at $\dot{\varepsilon} = 1.7 \times 10^{-3}$ s^{-1} is plotted as a function of temperature in Fig. 4. The maximum elongation occurs at around 450 °C and tends to reduce with increasing or decreasing temperature. Note, that at 490 °C, the elongation-to-failure of 120% corresponds with the largest value of the coefficient m equal to 0.7. This fact can be interpreted in terms of partial melting of the 7055 alloy at this temperature [6].

It is worth noting that the m value tends to decrease continuously with strain (Fig. 5). For instance, at 450 °C and at $\dot{\varepsilon} = 1.7 \times 10^{-3}$ s^{-1}, the coefficient of strain rate sensitivity drops from $m = 0.58$ at $\varepsilon = 0.34$ to $m = 0.32$ at $\varepsilon = 2$.

Microstructural evolution

The microstructural evolution of the 7055 alloy was examined under conditions of static annealing (grip section) and superplastic deformation (i.e. dynamic annealing in gauge section). Grain sizes observed from static annealing, L_s, dynamic annealing, L_d, and grain aspect ratio (AR), are summarized in Tables 1 and 2. The samples were deformed up to $\varepsilon = 1.1$ and up to failure in the temperature range 400–490 °C at a strain rate of 1.7×10^{-3} s^{-1}. It was found that static annealing and superplastic

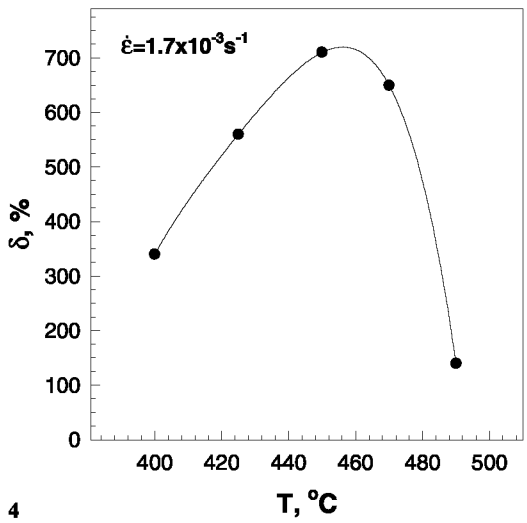

4

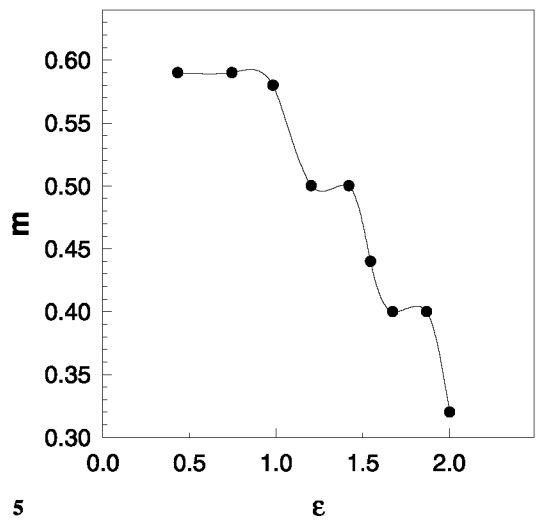

5

Fig. 4. Tensile elongation as a function of deformation temperature ($\dot{\varepsilon} = 1.7 \times 10^{-3}$ s^{-1}).
Fig. 5. Effect of strain on the coefficient of strain rate sensitivity at 450 °C and $\dot{\varepsilon} = 1.7 \times 10^{-3}$ s^{-1}.

Table 1
Average grain sizes, L_s and L_d, after static annealing and superplastic deformation (i.e. dynamic annealing) and volume fractions of recrystallized and unrecrystallized structures in the samples strained up to $\varepsilon = 1.1$ at a strain rate of 1.7×10^{-3} s^{-1} under various temperatures

	$T = 400$ °C	$T = 425$ °C	$T = 450$ °C	$T = 470$ °C
L_s (μm)	11.2	11.5	11.7	12.3
Volume fraction of unrecrystallized regions after static annealing	24	22	21	14
L_d (μm)[a]				
Recrystallized regions	12.3/9	16/11.2	19.1/14	14/11.3
Unrecrystallized regions	5.6/5.3	7.5/6.1	8.6/6.2	–
Volume fraction of unrecrystallized regions after superplastic deformation (%)	22	21	12	–

[a] Numerator and denominator are grain sizes measured in the longitudinal and transverse directions, respectively.

Table 2
Average grain sizes, L_s and L_d, after static annealing and superplastic deformation for the samples strained up to failure at a strain rate of 1.7×10^{-3} s^{-1} and at different temperatures

	$T = 400$ °C	$T = 425$ °C	$T = 450$ °C	$T = 470$ °C	$T = 490$ °C
Local strain in the area examined, (the period of equivalent exposure time h)	$\varepsilon = 1.5$ (1.1)	$\varepsilon = 1.9$ (1.4)	$\varepsilon = 2.1$ (1.7)	$\varepsilon = 2$ (1.6)	$\varepsilon = 0.9$ (0.7)
L_s (μm)	11.2	13.7	14.0	15.0	14.9
L_d (μm)[a]	14.4/9.1	15.4/12.0	17.7/13.0	19.7/16.0	17.6/13.9
AR of grains	1.58	1.28	1.36	1.23	1.26

[a] Numerator and denominator are grain sizes measured in the longitudinal and transverse directions, respectively.

deformation result in different microstructural changes at all temperatures examined. Static annealing leads to a slight decrease in the volume fraction of the unrecrystallized regions, and also a grain growth takes place in the recrystallized regions (Fig. 6a, Tables 1 and 2). There is almost no change in the crystallite size in the unrecrystallized regions.

It is apparent from Fig. 6b and c that superplastic deformation results in gradual transformation of subgrains in the unrecrystallized regions into grains surrounded by high angle boundaries. The latter can be evident from enhanced contrast of etched boundaries of crystallites. In addition, this conclusion was supported by data of orientation imaging microscopy which will be presented in future. A temperature increase accelerates this process. Volume fraction of unrecrystallized structure at a fixed strain decreases with increasing temperature (Table 1). An evidence for unrecrystallized structure was found at $\varepsilon \leqslant 1.1$ in the temperature range 400–450 °C (Fig. 6b and Table 1). With further deformation the unrecrystallized structure almost disappears (Fig. 6c and Table 2). At higher strains, only grains surrounded by high-angle boundaries are observed. At 470 °C, no unrecrystallized structure was observed after $\varepsilon = 1.1$.

Superplastic deformation results in a grain elongation along the tension axis, and a grain growth takes place in the both recrystallized and unrecrystallized regions. The

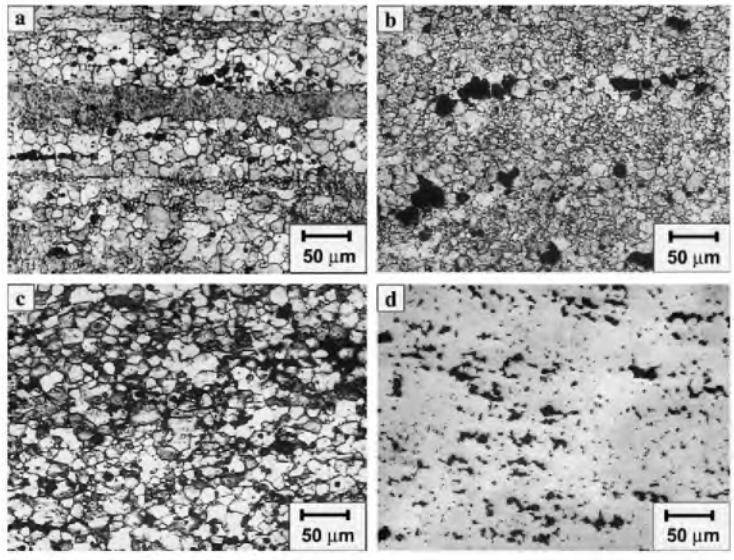

Fig. 6. Microstructures evolved during deformation at 450 °C and at $\dot{\varepsilon} = 1.7 \times 10^{-3}$ s^{-1} (a) grip section, annealing time is 1.7 h, (b) $\varepsilon = 1.1$, (c) and (d) $\varepsilon = 2.1$.

grain growth in the unrecrystallized regions is much faster than that in the recrystallized ones. For instance, in the recrystallized regions the grain size in the longitudinal direction is increased by 1.7 times at 450 °C, while that is increased by 4.3 times in the unrecrystallized regions. Therefore, transformation of subgrains into grains is accompanied by an extensive growth of these crystallites. As showed in Tables 1 and 2 an increase in temperature leads to a gradual grain growth with increasing strain. It can be noted, however, the grain structure of the 7055 Al is essentially stable under superplastic deformation.

Cavitation during superplastic deformation at a strain rate of 1.7×10^{-3} s^{-1} and different temperatures was examined on specimens deformed both up to $\varepsilon = 1.1$ and up to failure (Table 3). Cavitation in the fractured specimens was analyzed in an area 5 mm

Table 3
Average cavity size A, and porosity volume fraction V, for the 7055 alloy strained at $\dot{\varepsilon} = 1.7 \times 10^{-3}$ s^{-1} up to $\varepsilon = 1.1$ and up to failure under various temperatures

	$T = 400$ °C	$T = 425$ °C	$T = 450$ °C	$T = 470$ °C	$T = 490$ °C
$\varepsilon = 1.1$					
A (μm)	5.5	4	9	11	–
V (%)	1.4	0.6	2.4	3.7	–
Deformation up to failure					
Local true strain in areas examined	1.5	1.9	2.1	2	0.9
A (μm)	5.6	3.9	7.9	8.8	24.2
V (%)	1.5	3.9	9.8	5.5	7.8

apart from the fracture surface. The majority of large cavities was observed to grow along the tensile direction and to show an irregular and jagged shape (Fig. 6d) suggesting plasticity-controlled cavity growth [7]. These pores comprise chains along boundaries separating the two regions. Cavity interlinkage was also found in the transverse direction. Notably the average size of cavities tends slightly to reduce with strain, although it is quite unusual. In the temperature range 400–490 °C the volume fraction of porosity increases with increasing temperature from 1.5% at 400 °C to 9.8% at 450 °C in the samples strained up to failure (Table 3). Further increasing temperature leads to a decrease in the volume fraction of cavities to 5.5% at 470 °C. An extensive cavitation occurs during deformation at 490 °C.

The present experimental results can be summarized as follows. A partially recrystallized structure consisting of grains with a mean size of 11 μm and recovered subgrains with a mean size of 2 μm was produced in the 7055 alloy by the two-step TMP. The 7055 alloy with such microstructure exhibits superplasticity in the temperature interval 400–490 °C with a maximum total elongation of 960% and the coefficient $m = 0.6$ at 450 °C and $\dot{\varepsilon} = 3.3 \times 10^{-4}$ s^{-1}. At this temperature, the optimal interval of superplasticity occurs at 8.3×10^{-5}–8.3×10^{-3} s^{-1}. Such superplastic properties are superior to those of commercial aluminum alloys. Continuous dynamic recrystallization occurs during superplastic deformation and provides transformation of subgrain structure into granular structure in the unrecrystallized regions. The 7055 Al exhibits unusual cavitation behavior.

References

[1] Fridlyander, I. N. (2001). Met Sci Heat Treat 1, 5.

[2] Nieh, T. G., Wadsworth, J., & Sherby, O. D. (1996). Superplasticity in Metals and Ceramics (p. 210). New York: Cambridge University Press.

[3] Kaibyshev, O. A. (1992). Superplasticity of Alloys, Intermetallides, and Ceramics (p. 316). Berlin: Springer.

[4] Wert, J. A., Paton, N. E., Hamilton, C. H., & Mahoney, M. W. (1981). Metall Trans A 12, 1267.

[5] Chakrabarti, D. J. (1998). Superplasticity and Superplastic Forming (p. 155). Warrendale: TMS.

[6] Koike, J., Mabuchi, M., & Higashi, K. (1995). Acta Metall Mater 43, 199.

[7] Čadek, J. (1984). Creep in Metallic Materials (p. 302). Prague: Academia Press.